ISSN 1063-7745, Crystallography Reports, 2020, Vol. 65, No. 4, pp. 508–514. © Pleiades Publishing, Inc., 2020.
Russian Text © The Author(s), 2020, published in Kristallografiya, 2020, Vol. 65, No. 4, pp. 515–521.

DIFFRACTION AND SCATTERING OF IONIZING RADIATIONS

Theory of the Laue Diffraction of X Rays in a Thick Single Crystal with an Inclined Step on the Exit Surface. I: Numerical Solution

V. G. Kohn[a] and I. A. Smirnova[b,*]

[a] *National Research Centre "Kurchatov Institute," Moscow, 123182 Russia*
[b] *Institute of Solid State Physics, Russian Academy of Sciences, Chernogolovka, Moscow oblast, 142432 Russia*
**e-mail: irina@issp.ac.ru*

Received October 24, 2019; revised November 26, 2019; accepted November 27, 2019

Abstract—A method for computing the Laue diffraction of an X-ray spherical wave in a single crystal with an inclined step on the exit surface has been developed. The method is based on the use of two approaches to solving the problem: Fourier transformation of the wave function angular dependence in the case of a plate-shaped crystal and a numerical solution of the Takagi equations in the step area, where the diffraction parameters depend on the coordinate along the crystal surface. The effect of strong increase in the reflected-beam intensity (by a factor of more than 7 in the maxima) in the transition area, if the step boundary makes a smaller angle with the reflected-beam direction, is predicted based on the numerical calculations. The dependence of the effect on the step-boundary inclination angle is analyzed.

DOI: 10.1134/S1063774520040112

INTRODUCTION

Laue diffraction of an X-ray spherical wave in a plate-shaped single crystal is observed when the reflected beam exits from the sample through the same surface as the transmitted beam. This surface is referred to as the exit surface. This diffraction was experimentally observed for the first time in 1959 [1]. Coherent images were obtained in [1] using a narrow slit installed before the crystal, which, in fact, served as a secondary radiation source with a small cross section. This experimental method, which has been widely used for many years to study the quality of single crystals, is referred to as X-ray section topography.

The theory describing the experimental scheme [1] was developed in [2, 3] for zero source–crystal distance. An incident spherical wave was presented as a superposition of plane waves using Fourier transformation. The angular dependence of the transmission and reflection amplitudes in the case of plane-wave diffraction is determined analytically. It was found that the diffraction pattern on the exit crystal surface is observed in the Borrmann triangle formed by the incident and reflected beams. Then this pattern is transferred without changes to the detection plane.

Almost simultaneously, Takagi [4] proposed another version of the theory, which is based on a system of differential equations. Now, these equations are named after their discoverer. A numerical solution of the Takagi equations makes it possible to consider not only an arbitrary type of incident wave but also the lattice distortions near defects, as well as crystals of arbitrary shape. The system of differential equations for a perfect crystal has a solution in the form of a convolution of the wave function on the crystal boundary with the crystal propagator, which is expressed analytically in terms of Bessel functions. Various solutions for crystals with different boundaries and reflection geometries were obtained in [5–11].

A generalized theory of spherical-wave diffraction, where the source–detector distance was additionally taken into account, was developed in [12–14]. One of its main results was the prediction of the diffraction focusing of divergent radiation by a plate-shaped crystal. This effect was experimentally verified in [15–18].

An efficient numerical method was proposed to solve the Takagi equations for crystals containing structure defects (see, e.g., [19]) and calculations for different defects under different irradiation conditions were carried out [20]. The inhomogeneous structure of radiation upon diffraction in crystals of specific shape (parallelepiped or cylinder) was investigated both analytically and numerically in [21–27].

The purpose of this study was to investigate theoretically the diffraction of a spherical X-ray wave in a thick perfect crystal with an inclined step on the exit surface. Two approaches were used to solve the problem: Fourier transformation of the angular dependence of the wave function of a plane wave incident on a plate-shaped crystal and numerical solution of the Takagi equations in the step area, where the diffraction parameters depend on the coordinate along the sample surface. The analytical solution to the Takagi equa-

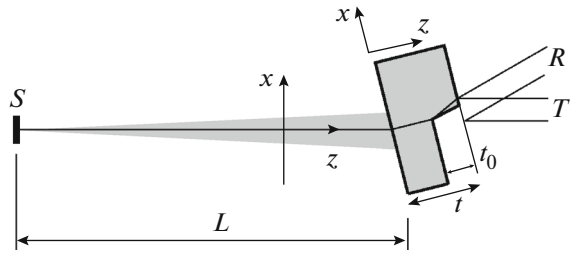

Fig. 1. Schematic of the calculation experiment: *S* is the spherical-wave source, *R* is the reflected beam, and *T* is the transmitted beam. The coordinate systems on the left and on the right correspond to the first and second stages of problem solution, respectively.

tions is reported in the second part of the work [28]. The interest in this sample shape is stems from the following fact: if the step inclination angle is smaller than the Bragg angle, the almost homogeneous spatial distribution of reflected-beam intensity changes significantly in the narrow transition area of the thick crystal (the intensity in the maximum increases by a factor of more than 7). This effect depends only slightly on the source–crystal distance, except for the diffraction-focusing region. The dependence of the effect on the step inclination angle has been analyzed. The results obtained stimulate experimental study of the effect and can be used for different practical purposes (in particular, for high-precision determination of the diffraction parameters depending on the crystal structure).

FORMULATION OF THE PROBLEM AND NUMERICAL SOLUTION TECHNIQUE

A schematic of the numerical experiment is shown in Fig. 1. A monochromatic spherical wave from a point X-ray source, located at a distance L from the single crystal, is incident on the crystal surface at the Bragg angle and has a finite angular divergence. The crystal is plate-shaped and has a thickness t (maximum thickness); there is an inclined step of height t_0 on its exit surface.

This formulation of the problem stems from the fact that the correct description of an X-ray source (synchrotron or a laboratory source) requires independent consideration of each point of the source cross section, because both electrons on the orbit of synchrotron source and atoms of the X-ray tube anode emit spontaneously, and there is no correlation between these microsources. The radiation, being monochromatizied in standard ways, does not affect the shape of the incident-wave cross section. The monochromator is omitted in Fig. 1. The effective transverse source size is taken into account by summing up the intensities of all cross section points.

The inclined step on the single-crystal exit surface leads to a spatial inhomogeneity of the intensities of transmitted and reflected beams in the cross section. The detectors measure these beams independently. They are spaced by a short distance to provide spatial separation of the beams and eliminate interference. For simplicity, we will calculate the beam intensities on the exit crystal surface in its thick part (thickness t).

It is convenient to divide the problem into two stages. In the first stage, we will calculate the wavefield distribution over the crystal thickness $t_1 = t - t_0$. The step is absent in this region, and the crystal is homogeneous along the surface (along the x axis). An intensity inhomogeneity occurs only due to the incident-wave inhomogeneity and the diffraction effect. In this case, it is convenient to solve the problem by the Fourier transform method, using the analytical solution for an incident plane wave.

Let us assume that the relativistic effects limit only slightly the beam angular divergence, and there is no need to introduce corrections into the Fresnel propagator, as was made in [29]. Within the paraxial approximation, it is convenient to write the wave function of the incident wave in the form

$$E_i(x) = (\lambda L)^{1/2} \exp(iKz) P(x, L), \quad (1)$$

where the z coordinate is counted from the source to the crystal (Fig. 1, axes on the left), λ is the X-ray wavelength, $K = 2\pi/\lambda$, and the Fresnel propagator can be written as

$$P(x, z) = (i\lambda z)^{-1/2} \exp\left(i\pi \frac{x^2}{\lambda z}\right). \quad (2)$$

The intensity is independent of the y coordinate in the direction perpendicular to the diffraction plane. Let us present (1) in the form of a Fourier integral over q and take into account that $q = K\theta$ describes a small angular divergence of incident radiation near the Bragg angle (i.e., the incident wave is a superposition of plane waves with the wave vector $\mathbf{k}_0 = (q, 0, K)$).

We consider the symmetric Laue diffraction from a system of atomic planes corresponding to the reciprocal-lattice vector $\mathbf{h}$. It is known that the wave vector of a transmitted wave does not change in the case of diffraction from a plate-shaped perfect crystal [20, 30]. Using the analytical solution for a plane wave, one can obtain directly a solution for the first stage in the form

$$E_0(x, t_1) = (\lambda L)^{1/2} \int \frac{dq}{2\pi} \exp(iqx) P(q, L) A_0(q, t_1). \quad (3)$$

Hereinafter, the factor $\exp(iKz)$ is omitted, because it does not affect the intensity. The analytical expression of the Fourier transform of Fresnel propagator has the form

$$P(q, z) = \exp\left(-i \frac{\lambda z}{4\pi} q^2\right), \quad (4)$$

and the solution to the problem for a plane wave is well known [20, 30, 31]. Let us write this solution in the form convenient for calculations:

$$A_0(q,t) = \frac{\exp(M+G) + r^2\exp(M-G)}{1+r^2}, \quad (5)$$

where

$$M = i[X_0 + \alpha_q]\frac{t}{2\gamma_0}, \qquad G = ig\frac{t}{2\gamma_0}, \quad g = (\alpha_q^2 + X^2)^{1/2}, \quad (6)$$

$$r = \frac{\alpha_q + g}{X}, \quad X_0 = K\chi_0, \quad X = K(\chi_h\chi_{-h})^{1/2}, \quad (7)$$

$$\alpha_q = (q - q_0)\sin 2\theta_B, \quad \gamma_0 = \cos\theta_B. \quad (8)$$

The parameter g has a positive imaginary part; χ_0, χ_h, and χ_{-h} are the Fourier components of the crystal polarizability for the reciprocal-lattice vectors 0, **h**, and −**h**, respectively; θ_B is the Bragg angle; and the parameter $q_0 = K\theta_0$ describes a possible deviation of crystal orientation from the Bragg angle.

A similar solution can be derived for the reflected wave:

$$E_h(x,t_1) = (\lambda L)^{1/2}\int\frac{dq}{2\pi}\exp(iqx)P(q,L)A_h(q,t_1), \quad (9)$$

where

$$A_h(q,t) = \frac{X_h}{2g}[\exp(M+G) - \exp(M-G)]. \quad (10)$$

Here, $X_h = K\chi_h$. In this case, the wave vector of plane waves is $\mathbf{k}_0 + \mathbf{h}$, and the reflected wave propagates along the direction making a double Bragg angle with the transmitted-wave direction.

In the second stage, we will solve another problem: diffraction in a plate-shaped crystal in the case of an arbitrary incident wave and arbitrary inhomogeneity of crystal structure in the xz plane. In this stage, we will use the another coordinate system (Fig. 1, on the right). The x and z axes are oriented along the plate surface and normally to the surface, respectively. The following Takagi equations will be numerically solved [4]:

$$\frac{2}{i}\frac{\partial E_0}{\partial s_0} = X_0E_0 + X_{-h}E_h\exp(i\mathbf{hu}), \quad (11)$$

$$\frac{2}{i}\frac{\partial E_h}{\partial s_h} = [X_0 + 2\alpha_q]E_h + X_hE_0\exp(-i\mathbf{hu}). \quad (12)$$

Here, $X_{-h} = K\chi_{-h}$; s_0 and s_h are the coordinates along the propagation directions of transmitted and reflected waves, respectively; and **u** is the shear vector due to possible lattice strain. The parameter of deviation from the Bragg condition, α_q, was determined in (8).

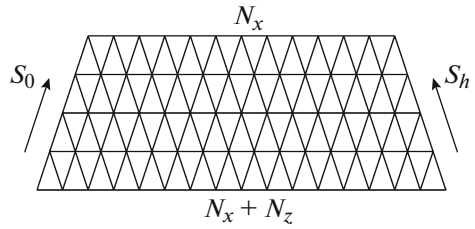

Fig. 2. Computational grid used in numerical solution of the Takagi equations and directions of oblique coordinate axes.

To solve the Takagi equations for the Laue diffraction, it is convenient to make a substitution $E_h = E_h'\exp(-i\mathbf{hu})$ and write the equation in the form

$$\frac{p}{2}\frac{\partial E_0}{\partial s_0} = U_0E_0 + UE_h', \qquad \frac{q}{2}\frac{\partial E_h'}{\partial s_h} = [V_0 + W]E_h' + VE_0, \quad (13)$$

where

$$U_0 = \frac{ip}{4}X_0, \quad U = \frac{ip}{4}X_{-h}, \quad V_0 = \frac{iq}{4}X_0, \quad (14)$$

$$V = \frac{iq}{4}X_h, \quad W = \frac{iq}{2}\left[\alpha_q + \frac{d\mathbf{hu}}{ds_h}\right]. \quad (15)$$

The parameters p and q are determined by approximate solution of the Takagi equations. We will consider the layers in the crystal of thickness d_z that are oriented parallel to the x axis. The parameters p and q are equal to the segments along the propagation directions of the transmitted and reflected waves, respectively, corresponding to a single layer. For symmetric diffraction, $p = q = d_z/\gamma_0$. In this model, there are no strains in the crystal (i.e., $\mathbf{u} = 0$); however, the parameters U_0, U, V_0, and V depend on the x and z coordinates.

To solve numerically Eqs. (13), one must replace the derivatives by the ratio of differences. Using the method proposed in [19], one can calculate the derivatives and functions in the middle of the layer according to the following algorithm:

$$p\frac{df(x-p/2)}{dx} = f(x) - f(x-p), \quad (16)$$

$$2f(x-p/2) = f(x) + f(x-p). \quad (17)$$

Having replaced the derivatives and functions in Eq. (13) for the middle of each layer, according to the algorithm (16), (17), we obtain a system of linear equations for the amplitudes of transmitted and reflected waves for the system of points with periods d_z and $d_x = 2d_z\tan\theta_B$ along the z and x axes, respectively (Fig. 2).

The solution to this system ($E_2^{(n)}$) can be written as a product of matrix $M_{2,4}$ and vector $E_4^{(o)}$:

$$E_2^{(n)} = M_{2,4} \times E_4^{(o)}, \quad (18)$$

where

$$E_2^{(n)} = [E_0(s_0, s_h), E_h'(s_0, s_h)], \quad (19)$$

$$E_4^{(o)} = [E_0(s_0^-, s_h), E_h'(s_0^-, s_h), E_0(s_0, s_h^-), E_h'(s_0, s_h^-)], \quad (20)$$

$$M_{2,4} = \frac{1}{D}\begin{pmatrix} U_0^+W_1^-, UW_1^-, UV, UW_1^+ \\ U_0^+V, UV, U_0^-V, U_0^-W_1^+ \end{pmatrix}. \quad (21)$$

Here, $s_0^- = s_0 - p$, $s_h^- = s_h - q$,

$$U_0^\pm = 1 \pm U_0, \quad W_1^\pm = 1 \pm W_1, \quad (22)$$

$$W_1 = W + V_0, \quad D = U_0^-W_1^- - UV. \quad (23)$$

The solution technique is as follows. Let us begin from the entrance surface of the first layer, where the amplitudes E_0 and E_h' are known from the boundary conditions, and use (18) to find the corresponding values on the layer exit surface, which is the entrance surface for the next layer, etc. As a result, we obtain the values at all grid points (Fig. 2). The number of grid points N_x along the x axis decreases by unity at each iteration. Therefore, to find the solution in the area of size $N_x d_x$ along the x axis, one must know the boundary conditions in the area $(N_x + N_z)d_x$ and the total thickness of the crystal in the second part $t_0 = N_z d_z$ (Fig. 2), where N_z is the number of layers.

Matrix (21) is for a crystal with a strained lattice. If a crystal has amorphous regions, in which diffraction is absent, the matrix for these regions has the form

$$M_{2,4} = \frac{1}{D}\begin{pmatrix} U_1^+V_1^-, 0, 0, 0 \\ 0, 0, 0, U_1^-V_1^+ \end{pmatrix}, \quad (24)$$

where

$$U_1 = \frac{ip}{4}X_1, \quad V_1 = \frac{iq}{4}X_1, \quad D = U_1^-V_1^-; \quad (25)$$

$$U_1^\pm = 1 \pm U_1, \quad V_1^\pm = 1 \pm V_1, \quad X_1 = K\chi_1. \quad (26)$$

Here, χ_1 is the zero Fourier component of crystal polarizability in the amorphous region, which may have another chemical composition. In particular, this region may be a void ($\chi_1 = 0$). For the symmetric case, $V_1 = U_1$.

In this study, the solution to the problem in the first stage determines the boundary conditions for the second stage. Since the point grids used in different stages differ, the necessary values can be obtained by interpolation. In addition, the x axis of the first stage must be projected on the x axis of the second stage, taking into account that these axes make the Bragg angle. Specific calculations were performed for the silicon crystal, and the parameters χ_0, χ_h, and χ_{-h} were calculated using the on-line-program [32].

The computer program was written in the ACL language [33]. The Fourier integrals (3) and (9) were calculated using a fast Fourier transform procedure built-in in the ACL language. The code of this procedure in the Fortran language has been known since the middle of the last century as a part of the NAG library [34]. The number of points used in the calculations is $N = 16384$. The point-grid step d_x is specified; the step $d_q = Kd_\theta = 2\pi/(Nd_x)$, and the computational box Nd_q in the reciprocal space should be sufficiently large so as to make the integrand function zero at the box boundaries.

Note that the amplitude (5) is $\exp(iX_0t_1/2\gamma_0)$; it is nonzero in a thin crystal in the limit $|q| \to \infty$. In this study, the crystal is thick, the modulus of the aforementioned function is close to zero, and thus the problem is removed. It is also important to control the spatial position of the Borrmann triangle. Fourier integrals (3) and (9) for zero distance ($L = 0$) are nonzero only in the range $x < 0$, because the point $x = 0$ corresponds to all rays whose angular position is beyond the Bragg diffraction range. It is convenient to shift the origin of coordinates along the x axis so as to make it correspond to the middle of the Borrmann triangle. An additional shift at a distance of $x_s = -L\theta_0$ is required in the case of finite distance to correct the change in the Bragg direction at crystal angular displacement.

A correct choice of the beam center is especially important in the case of thick crystal, because, due to the Borrmann effect (anomalous transmission with minimum absorption), only the beam part corresponding to the middle of the Borrmann triangle passes through the crystal. The axis can easily be shifted by multiplying the integrand function by the factor

$$F(q) = \exp\left(iq[L\theta_0 - t_1\sin\theta_B + x_0\cos\theta_B]\right). \quad (27)$$

Here, a possible displacement x_0 of the step front edge with respect to the middle of the Borrmann triangle is additionally introduced. Just the step boundary beginning is chosen as the center of the x axis of the coordinate system.

RESULTS AND DISCUSSION

Figure 3 shows the calculated intensity distributions in the inhomogeneous part of crystal (i.e., the layer with step). The parameters are as follows: photon energy $E = \hbar\omega = 10$ keV ($\lambda = 0.124$ nm); source–crystal distance $L = 2$ m; thickness of the homogeneous crystal part $t_1 = 1$ mm; step height on the exit surface $t_0 = 0.2$ mm; the step tilt angle θ is determined from the condition $R = \tan\theta/\tan\theta_B = 0.5$; silicon crystal;

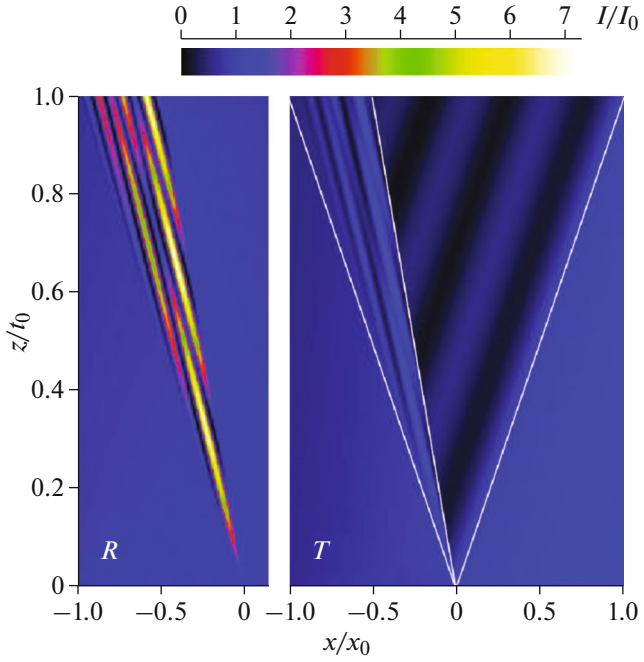

Fig. 3. Maps of the two-dimensional distributions of relative intensities of the reflected (left panel, *R*) and transmitted (right panel, *T*) beams in the step region; $t_0 = 0.2$ mm and $x_0 = 68.2$ μm.

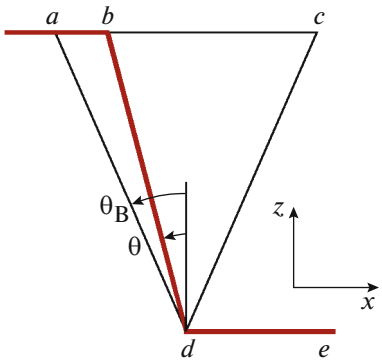

Fig. 4. Schematic diagram of the step and Borrmann triangle, with indication of regions characterized by different intensity distributions.

and reflection 220. Under these conditions $\theta_B = 18.84°$; therefore, $\theta = 9.68°$. The distance value used in the calculation, can easily be implemented experimentally using a narrow slit or a compound refractive lens, which form a secondary source at a desired distance.

Figure 4 shows a schematic diagram of the step boundary, with indication of the above-described angles. The step boundary corresponds to the line *abde*. This boundary changes the intensity inside the Borrmann triangle *acd*. The reflected-beam intensity *R* (Fig. 3, left panel) changes significantly only in the triangle *abd*, whereas the transmitted-beam intensity *T* (Fig. 3, right panel) changes within the entire Borrmann triangle (but differently in the regions *abd* and *bcd*). Both panels are presented on the same color scale for comparison convenience. The average reflected-beam intensity at the lower boundary (i.e., at the thickness t_1) is assumed to be unity. Note that the diffraction-focusing thickness [12, 36] for the distance under consideration is $t_{df} = L|\chi_h|F = 60.8$ μm, where $F = 1/(\sin\theta_B \sin 2\theta_B)$. Therefore, a part of radiation with weak absorption is maximally compressed at this thickness, then it diverges again, and exhibits an almost uniform intensity distribution over the *x* axis (along the surface) in the step region. In Fig. 3, the displacement $x_0 = 0$. The color map cannot reproduce very small changes in the intensity because of the absorption on the right from the step in the vertical direction. However, one can note weak changes in the transmitted-beam intensity in the horizontal direction. It can be seen in Fig. 3 that the transmitted-beam intensity in the Borrmann triangle near the step changes significantly (but not as radically as the reflected-beam intensity). In particular, the transmitted-beam intensity in the area *bcd* changes only along the direction transverse to the transmitted beam. In fact, it is transferred from the straight line *bd* in the transmitted-beam propagation direction. The intensity distribution in the area *abd* is more complex; however, the maximum intensity is much lower than the reflected-beam intensity in the same area.

The behavior of the reflected-beam intensity is most interesting. It has a pronounced interference character: the maximum exceeds the intensity before the step by a factor of about 7. One might suggest that this behavior is due to the fact that the step boundary is closer to the left side of the Borrmann triangle (i.e., to the reflected-beam direction). A very strong intensity redistribution, similar to the transmitted-wave reflection at the step boundary, can clearly be seen.

Figure 5 shows the dependences of the intensities averaged over a band equal to the Borrmann triangle base on the *z* coordinate in the step region for the transmitted beam (curve *1*), halved total intensity (curve *2*), and the reflected beam (curve *3*). The intensities are normalized with respect to the first point of curve *3* for the reflected beam. It can be seen that the average reflected-beam intensity even slightly increases. However, the average transmitted-beam intensity (curve *1*) drops sharply. The average total intensity of both beams (curve *2*) decreases linearly. For curve *2*, one can calculate the absorption coefficient along the normal to the surface: $\mu = 15.8$ cm^{-1}. For comparison, the normal absorption coefficient $\mu_0/\gamma_0 = 80.0$ cm^{-1} and the anomalous absorption coefficient for plane waves at the Bragg angle is $\mu_a/\gamma_0 = 2.5$ cm^{-1}. In other words, the step partially removes the conditions necessary for implementing the Borrmann effect. The total wave function of radiation is nonzero

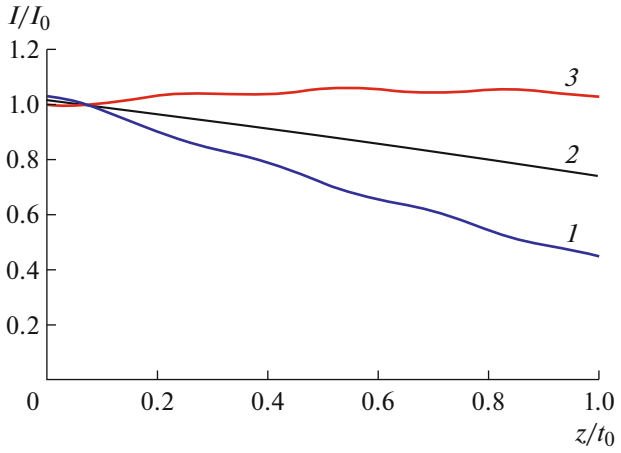

Fig. 5. Dependences of the average relative intensities on thickness in the step region for the (*1*) transmitted beam, (*2*) halved total intensity, and (*3*) reflected beam; t_0 = 0.2 mm.

at the location point of atoms, and the absorption increases. Note that the major part of the region under consideration does not contain any material, which corresponds to zero absorption. Absorption occurs mainly in the *abd* triangle. At the same time, the intensity is redistributed so that a part of transmitted-wave radiation is transformed into the reflected wave, which increases the reflected-wave intensity.

Figure 6 shows four fragments of the intensity distribution over the step height for different angles of inclination. Actually, the parameter R was varied, which took the following values: 0, 0.25, 0.5, and 0.75. All fragments are shown on the same color scale. It is of interest that the width of interference fringes decreases and their number changes only slightly with a decrease in the width of the transition region from the step boundary to the Borrmann triangle boundary. The highest maximum corresponds to the narrowest transition region. Moreover, in the narrow transition region, the oscillation period also shortens along the vertical axis, corresponding to the change in the crystal thickness.

This result can hardly be explained at the qualitative level. An analytical solution to this problem, yielding the same result, will be reported in the second part of the work. At the same time, the presence of interference fringes with a short period makes it possible to carry out precise measurements of various characteristics (including diffraction parameters).

Here, we considered the version with step inclination towards the reflected beam. When the step is inclined towards the transmitted beam, the roles of the transmitted and reflected beams change. In this case, patterns similar to those shown in Fig. 6 arise for the transmitted beam. This was demonstrated in [37], where a triangular cut on the exit surface was considered. The calculations show that the distributions in Figs. 3 and 6 barely depend on distance (they are almost the same at zero and extremely large distances). The only exceptions are the distances close to the diffraction-focusing length. For a 1-mm-thick crystal, this distance is 32.9 m.

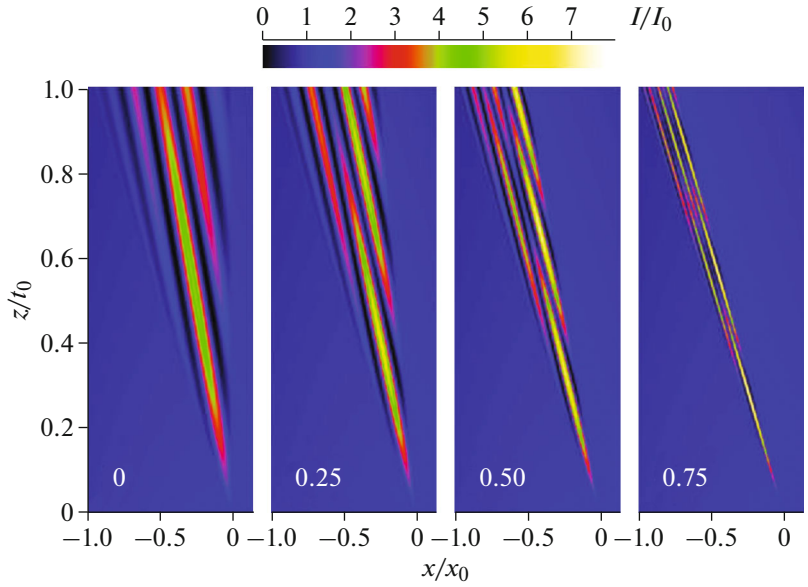

Fig. 6. Maps of two-dimensional distributions of reflected-beam relative intensities in the step region at different step inclination angles (t_0 = 0.2 mm and x_0 = 68.2 μm), with indication of the values of parameter $R = \tan\theta/\tan\theta_B$.

REFERENCES

1. N. Kato and A. R. Lang, Acta Crystallogr. **12**, 787 (1959).
2. N. Kato, Acta Crystallogr. **14**, 526 (1961); Acta Crystallogr. **14**, 627 (1961).
3. N. Kato, J. Appl. Phys. **39**, 2225 (1968).
4. S. Takagi, Acta Crystallogr. **15**, 1311 (1962).
5. I. Sh. Slobodetskii, F. N. Chukhovskii, and V. L. Indenbom, Pis'ma Zh. Eksp. Teor. Fiz. **8**, 90 (1968).
6. T. S. Uragami, J. Phys. Soc. Jpn. **27**, 147 (1969).
7. T. S. Uragami, J. Phys. Soc. Jpn. **28**, 1508 (1970).
8. T. S. Uragami, J. Phys. Soc. Jpn. **31**, 1141 (1971).
9. A. M. Afanas'ev and V. G. Kohn, Acta Crystallogr. A **27**, 421 (1971).
10. T. Saka, T. Katagawa, and N. Kato, Acta Crystallogr. A **28**, 102 (1972).
11. T. Saka, T. Katagawa, and N. Kato, Acta Crystallogr. A **28**, 113 (1972).
12. A. M. Afanas'ev and V. G. Kohn, Fiz. Tverd. Tela **19**, 1775 (1977).
13. V. G. Kohn, Kristallografiya **24** (4), 712 (1979).
14. V. G. Kohn, I. Snigireva, and A. Snigirev, Phys. Status Solidi B **222**, 407 (2000).
15. V. V. Aristov, V. I. Polovinkina, I. M. Shmyt'ko, and E. V. Shulakov, Pis'ma Zh. Eksp. Teor. Fiz. **28**, 6 (1978).
16. V. V. Aristov, V. I. Polovinkina, A. M. Afanas'ev, and V. G. Kohn, Acta Crystallogr. A **36**, 1002 (1980).
17. V. V. Aristov, V. G. Kohn, V. I. Polovinkina, and A. A. Snigirev, Phys. Status Solidi A **72**, 483 (1982).
18. V. D. Koz'mik and I. P. Mikhailyuk, Pis'ma Zh. Eksp. Teor. Fiz. **28**, 673 (1978).
19. Y. Epelboin, Acta Crystallogr. A **33**, 758 (1977).
20. A. Authier, *Dynamical Theory of X-ray Diffraction* (Oxford Univ. Press, New York, 2001).
21. N. M. Olekhnovich and A. I. Olekhnovich, Acta Crystallogr. A **34**, 321 (1978).
22. N. M. Olekhnovich and A. I. Olekhnovich, Acta Crystallogr. A **36**, 22 (1980).
23. D. K. Saldin, Acta Crystallogr. A **38**, 425 (1982).
24. T. S. Uragami, J. Phys. Soc. Jpn. **52**, 3073 (1983).
25. E. V. Shulakov, I. A. Smirnova, and E. V. Suvorov, Poverkhn.: Rentgenovskie, Sinkhrotronnye Neitr. Issled., No. 7, 32 (1996).
26. V. I. Punegov, S. I. Kolosov, and K. M. Pavlov, J. Appl. Crystallogr. **49**, 1190 (2016).
27. A. G. Shabalin, O. M. Yefanov, V. L. Nosik, et al., Phys. Rev. B **96**, 064111 (2017).
28. V. G. Kohn and I. A. Smirnova, Crystallogr. Rep. **65** (4), 515 (2020).
29. V. G. Kohn, J. Synchrotron Radiat. **25**, 1634 (2018).
30. Z. G. Pinsker, *Dynamical Scattering of X-Rays in Crystals* (Springer, Berlin, 1978).
31. V. G. Kohn, Phys. Status Solidi B **231**, 132 (2002).
32. http://kohnvict.ucoz.ru/jsp/3-difpar.htm.
33. http://kohnvict.ucoz.ru/acl/acl.htm.
34. https://www.nag.co.uk/content/nag-library-fortran.
35. A. Snigirev, V. Kohn, I. Snigireva, and B. Lengeler, Nature **384**, 49 (1996).
36. V. G. Kohn and I. A. Smirnova, Acta Crystallogr. A **74**, 699 (2018).
37. V. G. Kohn and I. A. Smirnova, Phys. Status Solidi B **257**, 1900441 (2020).

Translated by Yu. Sin'kov